

See discussions, stats, and author profiles for this publication at: <https://www.researchgate.net/publication/263582265>

# Modeling Air-to-Ground Path Loss for Low Altitude Platforms in Urban Environments

Conference Paper · December 2014

DOI: 10.1109/GLOCOM.2014.7037248

---

CITATIONS

20

READS

919

3 authors, including:



Akram Al-Hourani

RMIT University

26 PUBLICATIONS 118 CITATIONS

[SEE PROFILE](#)



Kandeepan Sithamparanathan

RMIT University

128 PUBLICATIONS 756 CITATIONS

[SEE PROFILE](#)

Some of the authors of this publication are also working on these related projects:



ABSOLUTE - Aerial Base Stations with Opportunistic Links for Unexpected and Temporary Events [View project](#)

All content following this page was uploaded by [Akram Al-Hourani](#) on 07 August 2014.

The user has requested enhancement of the downloaded file. All in-text references underlined in blue are added to the original document and are linked to publications on ResearchGate, letting you access and read them immediately.

# Modeling Air-to-Ground Path Loss for Low Altitude Platforms in Urban Environments

Akram Al-Hourani\* (*Student Member, IEEE*), Sithamparanathan Kandeepan\* (*Senior Member, IEEE*), and Abbas Jamalipour† (*Fellow Member, IEEE*)

\*School of Electrical and Computer Engineering, RMIT University, Melbourne, Australia.

†School of Electrical and Information Engineering, University of Sydney, Sydney, Australia.

Emails: {akram.hourani, kandeepan, a.jamalipour}@ieee.org

**Abstract**—The reliable prediction of coverage footprint resulting from an airborne wireless radio base station, is at utmost importance, when it comes to the new emerging applications of air-to-ground wireless services. These applications include the rapid recovery of damaged terrestrial wireless infrastructure due to a natural disaster, as well as the fulfillment of sudden wireless traffic overload in certain spots due to massive movement of crowds. In this paper, we propose a statistical propagation model for predicting the air-to-ground path loss between a low altitude platform and a terrestrial terminal. The prediction is based on the urban environment properties, and is dependent on the elevation angle between the terminal and the platform. The model shows that air-to-ground path loss is following two main propagation groups, characterized by two different path loss profiles. In this paper we illustrate the methodology of which the model was deduced, as well as we present the different path loss profiles including the occurrence probability of each.

**Index Terms**—Radio Propagation, Air-to-Ground, Low Altitude Platform, Aerial Base Station, Public Safety, Ray Tracing Simulation.

## I. INTRODUCTION

The recent developments in broadband wireless communication technology in terms of capacity and reliability has led an emerging rapid adoption by a wide sector of mission critical users, such as the public safety agencies including police forces and fire fighters. However, with the increasing dependency on such broadband networks, the total failure of public services would be massive if networks are disrupted due to a natural disaster such as flood, earthquake or tsunami, making the need for finding a rapid and cost-effective temporary recovery solution an important necessity.

One of the prospective feasible solutions for realizing wireless recovery networks, or as it is called in [1], [2] the *Emergency Supplementary Networks* (ESN) is by utilizing airborne base stations [3]. A concept that has been endorsed by the Homeland Security Bureau in USA as the *Deployable Aerial Communications Architecture* [4] envisions the recovery of critical communications for first responders within 12-18 hours. Another example of ESN development efforts is the ongoing European Commission funded project *ABSOLUTE* [5] focusing on Low Altitude Platforms (LAP).

When deploying an aerial network it is important to properly estimate the infrastructure required to establish the service [6], especially that radio resource and energy is quite limited in

such networks [7]–[9]. Accordingly, Radio Frequency (RF) planning should be carried out for the target area that can produce an estimation for the (i) the required number of Aerial Base Stations, (ii) the optimum altitude of the platforms [10], and (iii) the expected service level. In this paper, we propose a statistical RF propagation model for estimating the coverage of an Air-to-Ground wireless service provided by Low Altitude Platforms (LAP). The proposed radio model in this paper will allow aerial network operators to perform accurate RF planning without the need to rely on full site-specific ray tracing simulation. Since during the rush of the aftermath of a disaster it is unlikely that the city buildings 3D-model to be easily available. In this case the RF planning could be based on the urban statistical parameters that describes the city structures. These parameters are possible to obtain.

The call for proposing this generalized RF model was encouraged by two main motivations; (i) the increasing need for LAP-based wireless services [11], and (ii) the lack of a simple and generic statistical model that can easily link the urban statistical parameters with the radio propagation conditions. For example, authors in [12] are suggesting a method for finding the probability of a Line of Sight (LoS) between an aerial base station and a ground receiver as a function of the elevation angle, however no full shadowing model has been proposed. A step further was taken in [13] by building a path loss model based on three classes of links, Line of Sight (LoS), Obstructed Line of Sight (OLoS) and None Line of Sight (NLoS), however the study was based on a single model city, and cannot be widely generalized for different types of urban environments. While in [14] the approach was toward deducing a generic statistical model for air-to-ground path-loss that applies for a wide range of urban environment types, but the results were obtained for High Altitude Platforms only. In [15] a model based on Lonely-Rice propagation program was discussed, however it only accounts for large-scale terrain irregularities rather than addressing small scale urban environment properties. To the authors best knowledge there is no published work that is specifically addressing the path loss of low altitude platforms in different urban environments.

In this paper, we provide a generic radio model for predicting the path loss between a LAP and its corresponding ground

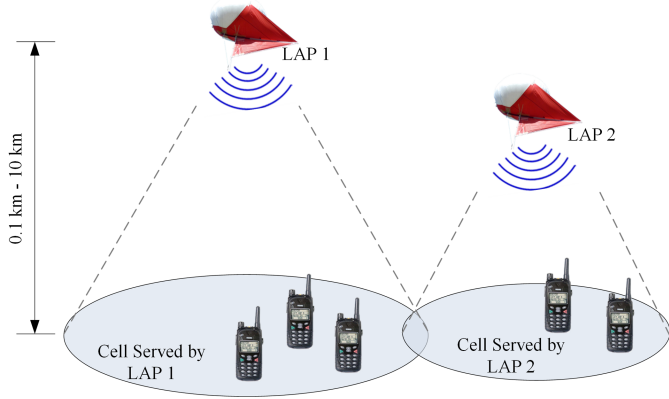


Fig. 1. Low altitude platform concept

receivers based on the urban environment statistical parameters of the target area. The following is the structure of this paper. In section II an overview of the Low Altitude Platform concept is illustrated, then urban environment modeling is discussed in section III, while section IV is dedicated for readers interested in the model development approach, after that, the implementation guidelines of the model are presented in section V and then section VI describes the applied verification method, followed by conclusion remarks in section VII.

## II. LOW ALTITUDE PLATFORMS

Low Altitude Platforms (LAP) [16] [17] are quasi-stationary aerial platforms (Quadcopters, UAVs or Balloons) with an altitude below the stratosphere (10,000 m), in contrary to High Altitude Platforms (Above 10,000 m) [18]. LAPs are much easier to deploy, and are more in line with the broadband cellular concept, since low altitude combines both coverage superiority and confined cell radius. For the RF model proposed here, we are focusing on the lower part of the stratosphere, i.e. for heights between 200m and 3,000m. The technology carried by the LAP depends on the end-user's application, budget and bandwidth requirements. Applications could be as advanced as LTE, Wi-Fi, WiMAX or as legacy as TETRA or P-25 systems.

Doppler Effect resulting from the possible high velocity of an airborne transmitter is not taken into consideration in this analysis, since the assumption is focusing on the quasi-stationary LAPs as represented in Figure 1.

## III. MODELING URBAN ENVIRONMENT

Developing an RF model requires an accurate definition of the study conditions and constraints; one of the most important conditions in an urban environment is the layout and characteristics of the buildings. The International Telecommunication Union (ITU-R) in its recommendation document [19], is suggesting a standardized model for urban areas, based on three simple parameters  $\alpha_o$ ,  $\beta_o$  and  $\gamma_o$ , that describe to a fair extent the general geometrical statistics of a certain urban area of which the RF signal propagates. These parameters are explained below:

- Parameter  $\alpha_o$ : Represents the ratio of built-up land area to the total land area (dimensionless).
- Parameter  $\beta_o$ : Represents the mean number of buildings per unit area (buildings/km<sup>2</sup>).
- Parameter  $\gamma_o$ : A scale parameter that describes the buildings heights distribution according to Rayleigh probability density function:

$$P(h) = \frac{h}{\gamma_o^2} \exp\left(\frac{-h^2}{2\gamma_o^2}\right) \quad (1)$$

where  $(h)$  is the building height in meters.

In order to cover a wide range of possible applications for this model, four simulation environments were selected, similar to [14]: (i) Suburban Environment that also covers the rural areas, (ii) Urban Environment which is the most common situation representing average European cities, (iii) Dense Urban Environment representing some types of cities where buildings are in close proximity to each other, (iv) Urban Environment with highrise buildings, representing modern cities with skyscrapers style. ITU-R statistical parameters are relatively straightforward to obtain from a certain city's urban plan, and are likely to be well documented by the city urban planning authorities. Table I, summarizes the selected ITU-R parameters for these environments.

TABLE I  
SELECTED URBAN ENVIRONMENTS

Environment	$\alpha_o$	$\beta_o$	$\gamma_o$
Suburban	0.1	750	8
Urban	0.3	500	15
Dense Urban	0.5	300	20
Highrise Urban	0.5	300	50

The challenge lies in finding a generic geometrical model that satisfies these parameters, and at the same time represents an acceptable layout of which a certain city might be structured. It is well known that for every city or suburb a certain urban planning code and style exists, so even if two cities share the same statistical parameters, that does not imply sharing the same buildings layout. Accordingly a "standard-city" plan should be modeled for allowing a valid general mathematical approximation. In this paper it has been selected to shape the virtual-city environment similar to Manhattan grid depicted in Figure 2; an array of structures (buildings or houses) of an assumed square plot of width  $W$ , and inter-building spacing of  $S$ . where  $W$  and  $S$  are measured in meters, and can be linked to the ITU-R statistical parameters, since by definition:  $\alpha_o = \frac{W^2 N_b}{(1000D)^2}$ , where  $D$  is the map side measured in kilometers (for a square patch), and  $N_b$  is the number of building inside the patch. On the other hand  $\beta_o = \frac{N_b}{D^2}$ . Accordingly we can write the width expression  $W$  as the following:  $W = 1000 \sqrt{\frac{\alpha_o}{\beta_o}}$ . Looking at the map patch, we can also notice that  $D = \frac{S+W}{1000} \sqrt{N_b}$ , accordingly, the spacing  $S$  can be rewritten as the following:  $S = \frac{1000}{\sqrt{\beta_o}} - W$ , where

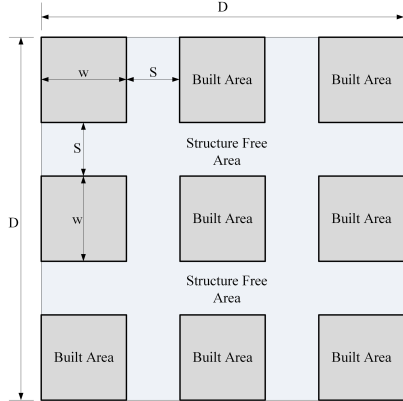


Fig. 2. The selected urban layout

$S$  includes all structure-free areas such as: pavements, roads, open gardens, open car parkings. Corresponding to the urban environment parameters listed in Table I, four virtual-cities were generated (using a script writing in MATLAB<sup>®</sup>), a city patch size of (1,000m × 1,000m) was selected for performing the radio propagation simulation. As depicted in Figure 3, building heights were randomly generated based on equation (1), while the width and spacing were kept constant for each of the generated environments. The plotted area in Figure 3 is limited to (250m × 250m) for a clearer representation.

Modeling urban environments does not only involve the geometry of the buildings but also should consider the materials and surface behavior of all structures, that will interact with electromagnetic (EM) waves generated by the LAP transmitter and will cause reflection, diffraction and scattering. Starting with reflection, the assumed material constituting the outer layer of the buildings was concrete, that has a non-negligible reflection and dielectric parameters [20]. While for scattering, all building edges were assumed as knife-edges, which is an acceptable idealization when developing RF propagation models [21], this approximation will allow a deterministic scattering calculation. Scattering effect resulting from surface irregularities was not considered.

Additional possible urban geometry effects of trees, lamp-posts and mobile objects reflections were neglected, assuming that the large-scale building geometry and its EM characteristics will dominate the average path loss. Buildings were considered as solid blocks, since it is unlikely that the propagation by penetration through buildings will have a significant effect on the model.

#### IV. RADIO MODEL DEVELOPMENT

When considering urban environments, RF signals are unlikely to travel via a single type of propagation method [22], since manmade structures introduce significant interactions with the radio path; such as signal blockage, diffraction, transmission and reflection. A ray tracing simulation (using 0.25° rays spacing) was conducted using Wireless InSite<sup>®</sup> ray tracing software for three types of rays (Direct, Reflected and Diffracted), while transmitted rays (through walls) were

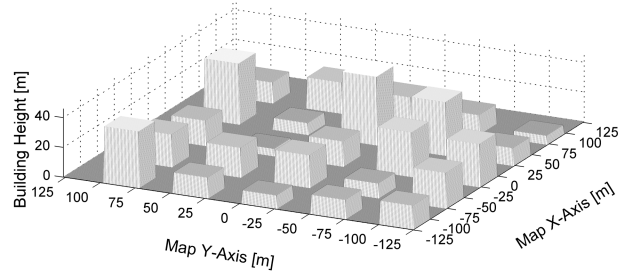


Fig. 3. Computer generated city models based on the ITU-R parameters.

neglected in order to simplify the calculations. As depicted in Figure 4, showing the direct rays, which are defined as signals traveled freely between the transmitter and the receiver with no obstacles' interaction. Receivers that can favor this type of rays are considered having full Line of Sight (LoS) condition with the transmitter. It is important to note that the availability of the geometrical line of sight does not necessarily mean that the RF line of sight condition is satisfied, since RF signals require much wider ellipsoids than the optical light, according to Fresnel Zones Concept [23]. The second treated rays type is the diffracted ones, which are considered a principle propagation mechanism in urban environments. In our simulation setup, we are considering the buildings as the only diffractive obstacles, where all edges are approximated to ideal knife-edges. In this case, the EM wave will follow a well-determined diffraction behavior. The third type of rays that might reach a receiver is by the means of reflection from buildings' walls, where each reflection causes a magnitude reduction in the electric field and a certain phase shift depending on the angle of incidence.

In order to obtain the coverage of the LAP over the target area (1,000m × 1,000m) we have simulated the received power of more than 37,000 uniformly distributed receivers, where the electric field of the all captured rays is summed (complex summation) and the received power is calculated from the resulting electric field. The total power loss impairing a signal transmitted from the LAP to  $n^{\text{th}}$  receiver can be written in decibel form as:

$$\text{PL}_n = 10 \log(P_{\text{TX}}) - 10 \log(P_{\text{RX}_n}) \quad (2)$$

where  $P_{\text{TX}}$  is the LAP transmitted power and  $P_{\text{RX}_n}$  is the received power at the  $n^{\text{th}}$  receiver. The simulated received power level is depicted in Figure 5, assuming a reference isotropic transmitter power of (0 dBm) placed 200m above the mean ground level. The ray tracing simulator will yield a list of all receivers including the corresponding path loss of each (we call these results as samples), and the samples are then further processed in order to obtain the excessive path loss component as we define it in the following formula:

$$\eta_n = \text{PL}_n - \text{FSPL}_n \quad (3)$$

where  $\text{FSPL}_n$  is the free space path loss for a certain receiver, obtained from Friis transmission equation [23] and represented

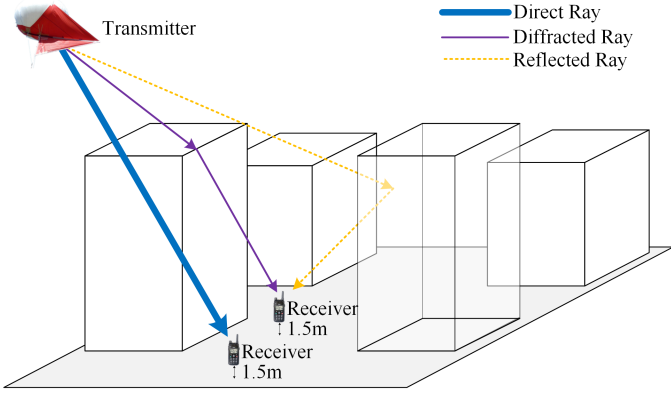


Fig. 4. The three different types of the simulated rays

as the following:

$$\text{FSPL}_n = 20 \log(d_n) + 20 \log(f_{\text{MHz}}) - 27.55 \quad (4)$$

where  $d_n = \left( \frac{\Delta h}{\sin \theta_n} \right)$  is the distance between the LAP and a receiver  $n$  measured in meters, and  $f_{\text{MHz}}$  is the system center frequency in MHz, accordingly:

$$\text{FSPL}_n = 20 \log \left( \frac{\Delta h}{\sin \theta_n} \right) + 20 \log(f_{\text{MHz}}) - 27.55 \quad (5)$$

where  $\Delta h = h_{\text{LAP}} - h_{\text{RX}}$ ;  $h_{\text{LAP}}$  is the LAP altitude and  $h_{\text{RX}}$  is the receivers' common height.  $\theta_n$  is the elevation angle (measured in degrees) as the LAP is seen from a certain receiver point. It is worthy to note that the LAP altitude itself has a minimal effect on the excessive part of the pathloss, where the main effect of the altitude resides in increasing the FSPL part [10].

The simulation is performed for three different frequencies (700 MHz, 2,000 MHz and 5,800 MHz) that are believed to cover a wide range of applications. Each frequency is simulated over the four different urban environments. The resulting data sets are 12 (3 frequencies  $\times$  4 environments).

#### A. Understanding Simulation Results

In order to understand the simulation results and deduce from them a radio model, we first obtain the data set histogram as depicted in Figure 6 showing the excessive path loss  $\eta$ . The histogram is showing a clear tendency towards three propagation groups, denoted as G1, G2 and G3, where (G1) the first group correspond to receivers favoring Line-of-Sight condition or near-Line-of-Sight condition, while (G2) the second group generally corresponds to receivers with no LAP Line-of-Sight but still receiving coverage via strong reflection and refraction, (G3) the third group has a very limited contribution to the total sample set, and corresponds to receivers suffering deep fading resulting from consecutive reflections and diffractions. In our model, we disregard the effect resulting from G3 as it constitutes less than 3% of the total samples set.

Samples clustering is then performed in order to study the statistical behavior separately for each propagation group by deducing the *mean value* and a *standard deviation* trend

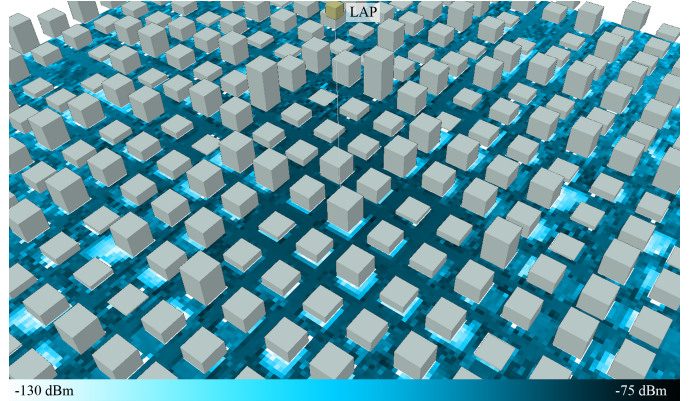


Fig. 5. Received Power, obtained at (Frequency = 2,000 MHz, Tx-Height = 200 m, Tx-Power = 0 dBm) for urban environment.

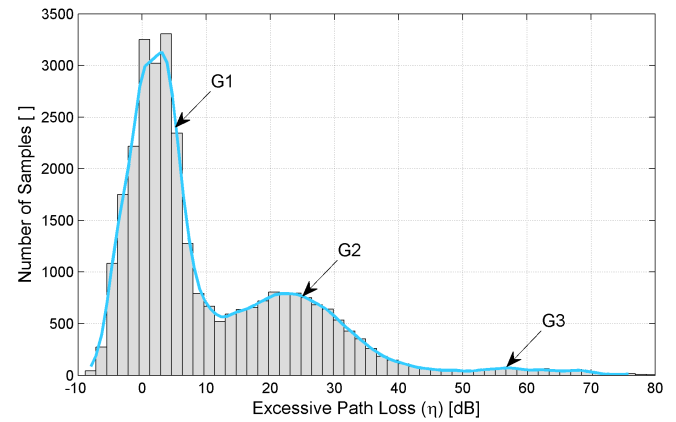


Fig. 6. Excessive path loss samples histogram, obtained at frequency = 2,000 MHz for a dense urban environment.

versus the available range of elevation angles, an example of samples clustering is depicted in Figure 7 showing the three propagation groups, while the density of samples was reduced by a factor of 10 for clearer depiction. It can be noticed from the figure that the samples tends to have a constant mean value (per group) for a certain frequency and urban environment, however samples distribution around the mean is taking more disperse values for lower elevation angles, and it is noticed that the standard deviation is angle dependent.

Finding parameters for the model requires fitting experimental data to explicit mathematical formulas. In order to do so, we define the *group occurrence probability* that represents the probability of a certain propagation group to occur at a certain elevation angle, and we denote it as  $p_\theta(\xi)$ , where  $\xi$  is the propagation group that a receiver could have, with two discrete values of either (1 or 2) as the third propagation group is ignored. Accordingly, at a particular elevation angle the excessive path loss will have a joint probability density function density function (PDF) of  $f_\theta(\eta, \xi)$  which can be expressed as:

$$f_\theta(\eta, \xi) = f_\theta(\eta|\xi) \cdot p_\theta(\xi) \quad (6)$$

where  $f_\theta(\eta|\xi)$  is the conditional PDF of  $\eta$  given  $\xi$ . An

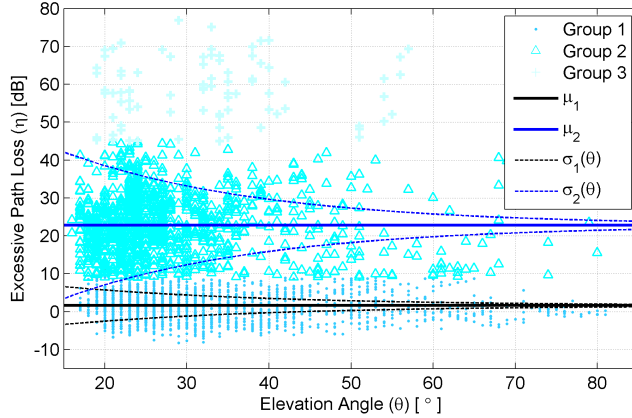


Fig. 7. Excessive path loss samples organized in terms of the elevation angle  $\theta$ , and categorized into three distinct propagation groups, obtained at frequency = 2,000 MHz for a dense urban environment.

illustrative representation of the excessive path loss PDF could be visualized by obtaining the integration of  $f_\theta(\eta, \xi)$  for all values of  $\theta$ , given by:

$$\int_{\theta} f_\theta(\eta, \xi) d\theta = f(\eta, \xi) \quad (7)$$

In order to simplify the mathematical modeling of the propagation group distribution  $f_\theta(\eta|\xi)$  we propose the use of Gaussian distribution model. Hence,  $f_\theta(\eta|\xi)$  can be expressed as the following:

$$f_\theta(\eta|\xi) = \mathcal{N}(\mu_\xi, \sigma_\xi^2(\theta)) \quad (8)$$

where  $\mathcal{N}$  is the normal distribution of a mean  $\mu_\xi$  and a standard deviation  $\sigma_\xi(\theta)$ . The remaining task is to find the model equations for  $p_\xi(\theta)$ ,  $\sigma_\xi(\theta)$  and  $\mu_\xi$ .

### B. Obtaining Radio Model Parameters

Starting with  $\mu_\xi$ , as stated previously the mean excessive path loss did not show a clear dependency on the elevation angle  $\theta$  but rather a constant value, that can be obtained by averaging all samples in a certain propagation group, the results are listed in Table II.

While for obtaining the general trend of the standard deviation of G1 and G2. We first obtain the standard deviation of each subset belonging to a common elevation angle and a common propagation group as discrete points depicted in Figure 8 as (triangles and squares). After that, the samples are fitted to the following formula:

$$\sigma_\xi(\theta) = a_\xi \exp(-b_\xi \cdot \theta) \quad (9)$$

where  $a_\xi$  and  $b_\xi$  are frequency and environment dependent parameters obtained by curve fitting using Damped Least-Squares (DLS) method, and are listed in Table II. As depicted in the same figure, the fitting of the standard deviation shows very good approximation.

For modeling  $p_\theta(\xi)$  we first count the number of samples occurred in a certain propagation group at a certain elevation angle  $K_\xi(\theta)$ , also we count the total number of samples having

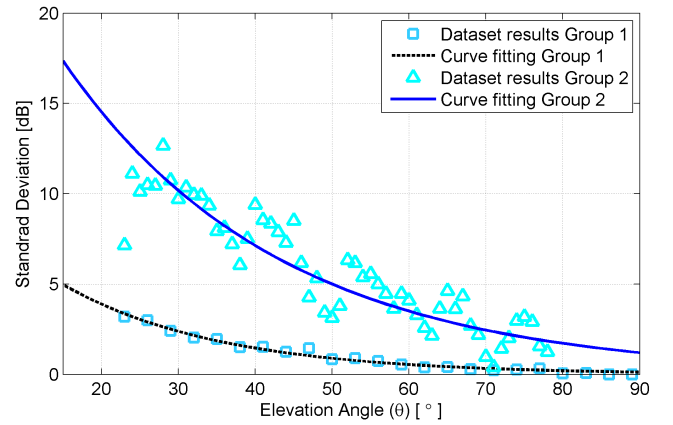


Fig. 8. Excessive Path Loss Standard Deviation, obtained at frequency = 2,000 MHz for an urban environment.

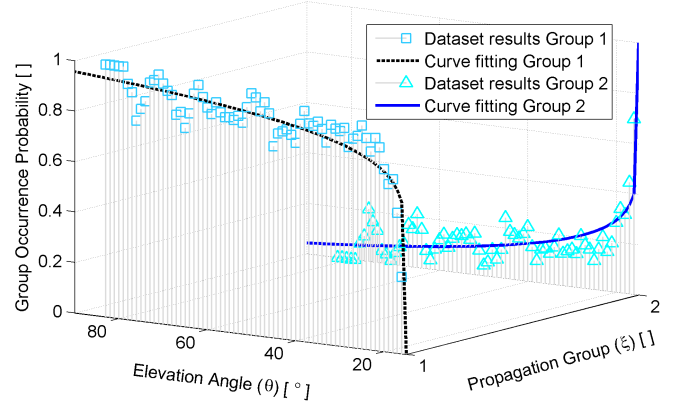


Fig. 9. Propagation Group Occurrence Probability, obtained at frequency = 2,000 MHz for an urban environment.

the same elevation angle  $K_{\text{Total}}(\theta)$ , then we calculate the following ratio:

$$\hat{p}_\theta(\xi) = \frac{K_\xi(\theta)}{K_{\text{Total}}(\theta)} \quad (10)$$

Equation (10) gives an estimation of the group occurrence probability  $p_\theta(\xi)$ , the estimation accuracy enhances for large sample sets. In this study we assume  $p_\theta(\xi) = \hat{p}_\theta(\xi)$  and accordingly we obtain the explicit form of  $p_\theta(\xi)$  using curve fitting of  $\hat{p}_\theta(\xi)$  points. In Figure 9 an example of a group occurrence curve fitting is illustrated for urban environment at frequency of 2,000 MHz for the two main distinct groups of propagation. The solid curves in the figure represent the probability of a certain propagation group to occur at a certain angle, that can be represented as:

$$p_\theta(\xi) = \int_{-\infty}^{+\infty} f_\theta(\eta, \xi) d\eta \quad (11)$$

while the discrete data points (triangles and squares) represent the measured ratio  $\hat{p}_\theta(\xi)$  as explained before.

It is important to note that the proposed model here is valid only for elevation angles above  $15^\circ$ , since low elevation angles have a very limited probability of receiving any signal from

the LAP, another reason is that the selected simulation setup can produce results for down to about  $15^\circ$  only.

The resulting curve explicit equation for group occurrence probability is chosen to balance simplicity and accuracy, and it is a function of the elevation angle as the following:

$$p_\theta(1) = c \cdot (\theta - \theta_o)^d \quad (12)$$

where  $\theta_o$  is selected as  $15^\circ$  corresponding to the minimum angle allowed by the model.  $c$  and  $d$  are frequency and environment dependent parameters obtained by curve fitting using (DLS) method. The results are listed in Table II.  $p_\theta(1)$  represents the probability of a signal to be received obeying group 1 path loss profile. On the other hand group 2 occurrence probability  $p_\theta(2)$  can be simply calculated as it is the complimentary of group 1 probability:

$$p_\theta(2) = 1 - p_\theta(1) \quad (13)$$

The three model parameters are now explicitly defined, the following section will demonstrate how to implement and utilize the proposed radio model.

TABLE II  
RF MODEL PARAMETERS

700 MHz				
	Suburban	Urban	Dense Urban	Highrise Urban
$\mu_1$	0.0	0.6	1.0	1.5
$\mu_2$	18	17	20	29
(a <sub>1,b<sub>1</sub></sub> )	(11.53, 0.06)	(10.98, 0.05)	(9.64, 0.04)	(9.16, 0.03)
(a <sub>2,b<sub>2</sub></sub> )	(26.53, 0.03)	(23.31, 0.03)	(30.83, 0.04)	(32.13, 0.03)
(c,d)	(0.77, 0.05)	(0.63, 0.09)	(0.37, 0.21)	(0.06, 0.58)

2,000 MHz				
	Suburban	Urban	Dense Urban	Highrise Urban
$\mu_1$	0.1	1.0	1.6	2.3
$\mu_2$	21	20	23	34
(a <sub>1,b<sub>1</sub></sub> )	(11.25, 0.06)	(10.39, 0.05)	(8.96, 0.04)	(7.37, 0.03)
(a <sub>2,b<sub>2</sub></sub> )	(32.17, 0.03)	(29.6, 0.03)	(35.97, 0.04)	(37.08, 0.03)
(c,d)	(0.76, 0.06)	(0.6, 0.11)	(0.36, 0.21)	(0.05, 0.61)

5,800 MHz				
	Suburban	Urban	Dense Urban	Highrise Urban
$\mu_1$	0.2	1.2	1.8	2.5
$\mu_2$	24	23	26	41
(a <sub>1,b<sub>1</sub></sub> )	(11.04, 0.06)	(10.67, 0.05)	(9.21, 0.04)	(7.15, 0.03)
(a <sub>2,b<sub>2</sub></sub> )	(39.56, 0.04)	(35.85, 0.04)	(40.86, 0.04)	(40.96, 0.03)
(c,d)	(0.75, 0.06)	(0.56, 0.13)	(0.33, 0.23)	(0.05, 0.64)

## V. RADIO MODEL IMPLEMENTATION

The proposed RF model here allows designers to calculate the expected path loss for receivers in a certain geographical area. Path loss information can be used to produce numerous information, such as the Signal to Interference and Noise Ratio (SINR), and the expected throughput. The design steps to implement this RF model are illustrated below:

- Get System Parameters (Center Frequency, LAP Altitude) and Urban Statistical Parameters  $\alpha_o$ ,  $\beta_o$  and  $\gamma_o$ .

- Select a receiver  $n$ .
- Calculate the Elevation Angle  $\theta$  of receiver  $n$ .
- Calculate the Free Space Path Loss of receiver  $n$  according to equation (5).
- Pick a propagation group randomly corresponding to the occurrence probability, using the *Group Randomization* method explained later.
- Generate the excessive path loss  $\eta$  of receiver  $n$  as a random number according to the mean and standard deviation of the corresponding propagation group.
- Calculate the total path loss of receiver  $n$  according to equation (2).
- Repeat steps 2 to 7 for all receiving points.

It is important to implement the Group Randomization correctly, the randomization should deduce the same probability of occurrence as per equations (12) and (13). And in order to facilitate the model implementation we suggest the following pseudocode for propagation groups randomization:

- Calculate groups occurrence probability as per equations (12) and (13):  $p_\theta(1)$ ,  $p_\theta(2)$ .
- Generate a random (RAND) number between 0 and 1, with uniform distribution.
- If  $p_\theta(1) \geq p_\theta(2)$  then If RAND  $\geq p_\theta(2)$  the propagation group is 1 otherwise it is group 2.
- Else if  $p_\theta(1) < p_\theta(2)$  then If RAND  $\geq p_\theta(1)$  the propagation group is 2 otherwise it is group 1.

Noticing that patch areas with dimensions larger than  $1\text{km} \times 1\text{km}$  can be split up into smaller divisions if needed, i.e. if the urban environment statistical parameters  $\alpha_o$ ,  $\beta_o$  and  $\gamma_o$  noticeably varies for each geographic sub-patch, then each sub-patch can be treated independently. Another point that should be taken into consideration is the directivity of the implemented antenna system, because the provided model is assuming isotropic transmitters and receivers.

## VI. RADIO MODEL VERIFICATION

The advancement of computer-aided propagation tools that are based on ray tracing simulation allows the prediction of signal strength in a very accurate manner [24] [25]. However as any other RF model, the accuracy lies in the stipulated mathematical assumptions, for example if the target area seems to follow an entirely different buildings layout than the one assumed here, then the accuracy of the model predictions will decrease. The aim of an RF model is to simplify simulation calculations and to speed up radio coverage estimation; however it cannot match the accuracy of site-specific ray tracing simulations. In order to verify the proposed RF model in this paper, we have compared the simulation data for a patch area of  $(1,000\text{m} \times 1,000\text{m})$  obtained from Wireless InSite® ray tracing simulator on one hand, versus the model parameters listed in Table II implemented using MATLAB® on the other hand. The obtained results are presented in terms of the cumulative distribution function versus the path loss (in dB). Figure 10, depicts the comparison results, showing high level of matching between the CDF curves. This matching

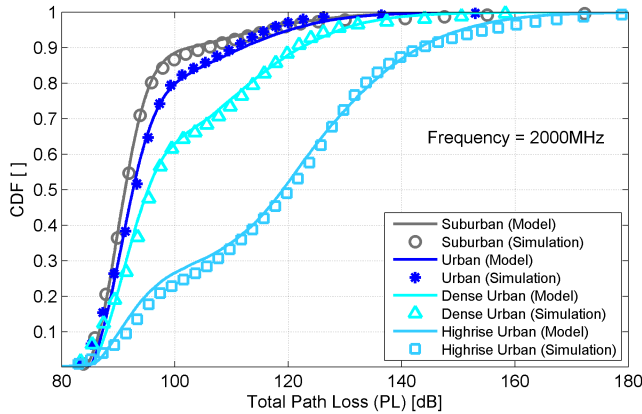


Fig. 10. Cumulative Distribution Function comparison between the proposed RF model vs. ray tracing simulation data.

indicates that the prediction resulting from the mathematical model reproduces the path loss estimations in an accurate manner with respect to the ray tracing simulation. Verification performed for the three model frequencies, while only F=2,000 MHz is depicted in the figure.

## VII. CONCLUSION

This paper provided a statistical generic Air-to-Ground RF propagation model for Low Altitude Platforms, that can substantially facilitate the planning efforts of airborne wireless services, since the RF planning can be performed based on merely simple urban parameters, rather than depending on site-specific 3D-models that are unlikely to be easily available and updated. The air-to-ground path loss showed a clear tendency towards two distinct propagation groups that were thoroughly discussed and analyzed for outdoor receivers. Future work will include the physical verification of the model by launching an actual LAP transmitter along with ground drive test setup, allowing the measurement of the received power in various locations, under several urban conditions. Also, a comprehensive study of Air-to-Indoor penetration will be conducted as part of a future work.

## ACKNOWLEDGMENT

The research was partially funded by the ABSOLUTE project from the European Commission's Seventh Framework Programme (FP7-2011-8) under the Grant Agreement FP7-ICT-318632 [5].

## REFERENCES

- [1] A. Al-Hourani and S. Kandeepan, "Cognitive Relay Nodes for airborne LTE emergency networks," in *7th International Conference on Signal Processing and Communication Systems (ICSPCS)*, Gold Coast, Australia, Dec 2013, pp. 1–9.
- [2] ——, "Temporary Cognitive Femtocell Network for public safety LTE," in *IEEE 18th International Workshop on Computer Aided Modeling and Design of Communication Links and Networks (CAMAD)*, Berlin, Germany, Sept 2013, pp. 190–195.
- [3] S. Kandeepan, K. Gomez, L. Reynaud, and T. Rasheed, "Aerial-Terrestrial Communications: Terrestrial Cooperation and Energy-Efficient Transmissions to Aerial-Base Stations," *IEEE Transactions on Aerospace and Electronic Systems*, Accepted, Feb 2014.
- [4] FCC, "The Role of Deployable Aerial Communications Architecture in Emergency Communications and Recommended Next Steps," *White Paper*, 2009. [Online]. Available: [http://hraunfoss.fcc.gov/edocs\\_public/attachmatch/DOC309742A1.pdf](http://hraunfoss.fcc.gov/edocs_public/attachmatch/DOC309742A1.pdf)
- [5] "EU-FP7 ICT IP Project ABSOLUTE," 2013. [Online]. Available: <http://www.absolute-project.eu/reports/publications>
- [6] K. Gomez, T. Rasheed, L. Reynaud, and S. Kandeepan, "On The Performance of Aerial LTE Base-Stations for Public Safety and Emergency Recovery," in *IEEE Globecom Workshops (GC Wkshps)*, Dec 2013, pp. 1391–1396.
- [7] S. Chandrasekharan, S. Kandeepan, R. Evans, A. Munari, R. Hermenier, M.-A. Marchitti, and K. Gomez, "Clustering Approach for Aerial Base-Station Access with Terrestrial Cooperation," in *IEEE Globecom Workshops (GC Wkshps)*, Dec 2013, pp. 1397–1402.
- [8] S. Kandeepan, K. Gomez, T. Rasheed, and L. Reynaud, "Energy Efficient Cooperative Strategies in Hybrid Aerial-Terrestrial Networks for Emergencies," in *IEEE 22nd International Symposium on Personal Indoor and Mobile Radio Communications (PIMRC)*, Sept 2011, pp. 294–299.
- [9] K. Gomez, S. Kandeepan, L. Reynaud, and T. Rasheed, "Adaptive Energy Efficient Communications for Rapidly Deployable Aerial-Terrestrial Networks," in *IEEE International Conference on Communications Workshops (ICC)*, June 2013, pp. 452–457.
- [10] A. Al-Hourani and S. Kandeepan, "Optimal LAP Altitude for Maximum Coverage," *IEEE Letters on Wireless Communications*, 2014.
- [11] L. Reynaud, T. Rasheed, and S. Kandeepan, "An Integrated Aerial Telecommunications Network that Supports Emergency Traffic," in *14th International Symposium on Wireless Personal Multimedia Communications (WPMC)*, Oct 2011, pp. 1–5.
- [12] Q. Feng, E. Tameh, A. Nix, and J. McGeehan, "Modelling the Likelihood of Line-of-Sight for Air-to-Ground Radio Propagation in Urban Environments," in *IEEE GLOBECOM '06*, 2006.
- [13] Q. Feng, J. McGeehan, E. Tameh, and A. Nix, "Path Loss Models for Air-to-Ground Radio Channels in Urban Environments," in *IEEE VTC 2006*, vol. 6, 2006, pp. 2901–2905.
- [14] J. Holis and P. Pechac, "Elevation Dependent Shadowing Model for Mobile Communications via High Altitude Platforms in Built-Up Areas," *IEEE Transactions on Antennas and Propagation*, vol. 56, no. 4, pp. 1078–1084, 2008.
- [15] M. Weiner, "Use of the Longley-Rice and Johnson-Gierhart Tropospheric Radio Propagation Programs:0.02–20 GHz," *IEEE Journal on Selected Areas in Communications*, vol. 4, no. 2, pp. 297–307, 1986.
- [16] S. Rohde and C. Wietfeld, "Interference Aware Positioning of Aerial Relays for Cell Overload and Outage Compensation," in *IEEE Vehicular Technology Conference (VTC Fall)*, 2012, pp. 1–5.
- [17] A. Valcarce, T. Rasheed, K. Gomez, S. Kandeepan, L. Reynaud, R. Hermenier, A. Munari, M. Mohorcic, M. Smolnikar, and I. Bucaille, "Airborne Base Stations for Emergency and Temporary Events," in *Personal Satellite Services*. Springer, 2013, pp. 13–25.
- [18] T. Tozer and D. Grace, "High-altitude platforms for wireless communications," *Electronics & Communication Engineering Journal*, vol. 13, no. 3, pp. 127–137, 2001.
- [19] ITU-R, "Rec. P.1410-2 Propagation Data and Prediction Methods for The Design of Terrestrial Broadband Millimetric Radio Access Systems," *P Series, Radiowave propagation*, 2003.
- [20] H. C. Rhim and O. Buyukozturk, "Electromagnetic Properties of Concrete at Microwave Frequency Range," *ACI Materials Journal*, vol. 95, no. 3, 1998.
- [21] ITU-R, "Rec. P.526-8, Propagation by Diffraction," *The ITU Radiocommunication Assembly*, 2003.
- [22] G. L. Stüber, *Principles of Mobile Communication*, 3rd ed. Springer, 2002.
- [23] A. Saakian, *Radio Wave Propagation Fundamentals*. Artech House, 2011.
- [24] V. Erceg, et al., "Comparisons of a Computer-Based Propagation Prediction Tool with Experimental Data Collected in Urban Microcellular Environments," *IEEE Journal on Selected Areas in Communications*, vol. 15, no. 4, pp. 677–684, 1997.
- [25] A. Al-Hourani, S. Chandrasekharan, and S. Kandeepan, "Path Loss Study for Millimeter Wave Device-to-Device Communications In Urban Environment," in *IEEE ICC'14 - Workshop on 5G Technologies, Sydney, Australia*.